

Accelerating Robotic Reinforcement Learning with Agent Guidance

Haojun Chen^{1,2†}, Zili Zou^{2†}, Chengdong Ma¹, Yaxiang Pu², Haotong Zhang^{1,2}, Yuanpei Chen^{1,2✉}
Yaodong Yang^{1,2✉},

¹Institute for Artificial Intelligence, Peking University, ²PKU-PsiBot Joint Lab

Abstract—Reinforcement Learning (RL) offers a powerful paradigm for autonomous robots to master generalist manipulation skills through trial-and-error. However, its real-world application is stifled by severe sample inefficiency. Recent Human-in-the-Loop (HIL) methods accelerate training by using human corrections, yet this approach faces a scalability barrier. Reliance on human supervisors imposes a 1:1 supervision ratio that limits fleet expansion, suffers from operator fatigue over extended sessions, and introduces high variance due to inconsistent human proficiency. We present Agent-guided Policy Search (AGPS), a framework that automates the training pipeline by replacing human supervisors with a multimodal agent. Our key insight is that the agent can be viewed as a semantic world model, injecting intrinsic value priors to structure physical exploration. By using executable tools, the agent provides precise guidance via corrective waypoints and spatial constraints for exploration pruning. We validate our approach on two tasks, ranging from precision insertion to deformable object manipulation. Results demonstrate that AGPS outperforms HIL methods in sample efficiency. This automates the supervision pipeline, unlocking the path to labor-free and scalable robot learning.
Project website: <https://agps-rl.github.io/agps>.

I. INTRODUCTION

Deep Reinforcement Learning (RL) [41, 6, 37] is a powerful paradigm for enabling autonomous robots to acquire general manipulation skills. RL allows agents to discover optimal policies without the constraints of hand-crafted modeling by leveraging trial-and-error interactions. However, the real-world application of RL is frequently hindered by low sample efficiency [34, 14].

To speed up learning, Human-in-the-Loop (HIL) methods [9, 29] are commonly used to guide robots. This approach works well for single tasks. However, it faces a “scalability barrier,” as shown in Figure 1. This barrier arises from a mismatch. Robot tasks become more complex, creating more situations to handle. But humans can only provide limited guidance. Each robot needs one person to supervise it. This makes it hard to expand to many robots. In addition, humans become tired during long training processes. Their guidance becomes less accurate and slower. Therefore, the need for supervision grows beyond what humans can provide. This prevents HIL from scaling to handle multiple tasks.

To overcome the limitations depicted in Figure 1, we need guidance that does not depend on human labor. We propose using multimodal agents. These agents can be viewed as semantic world models, injecting intrinsic value priors derived from internet-scale pretraining into the robotic system beyond

offering scalable supervision. The agents can use tools to apply this knowledge. By calling algorithms for spatial geometry and retrieving knowledge, the agents can identify task-relevant regions, thus pruning the search space. In this work, we present **Agent-guided Policy Search (AGPS)**, a framework that uses these capabilities to automate robot training. To bridge the frequency gap between high-speed RL interactions and low-frequency agent reasoning, we incorporate FLOAT [49], an online failure detector. FLOAT monitors the policy’s behavior in real-time and triggers the agent only when distribution drift occurs. Upon activation, the agent uses tools to provide supervision in two ways: (1) Action Guidance, which generates correct waypoints to recover from failures, and (2) Exploration Pruning, which defines explicit 3D spatial constraints to mask out task-irrelevant states.

We evaluate AGPS on two challenging real-world manipulation tasks spanning distinct physical properties: USB insertion, which demands high-precision control for rigid body assembly, and Chinese knot hanging, which requires intricate interaction with deformable linear objects. Across both domains, our results demonstrate that AGPS outperforms the HIL methods in sample efficiency with zero human intervention. In summary, this work makes two main contributions. **First**, we propose AGPS, a framework that automates RL supervision by integrating a multimodal agent with the FLOAT trigger mechanism to balance inference cost and sample efficiency. **Second**, we demonstrate that AGPS significantly outperforms baselines without human in the loop through real-world experiments.

II. PRELIMINARIES

This section introduces the reinforcement learning framework and Optimal Transport (OT) [36] for failure detection.

A. Reinforcement Learning

We model the manipulation task as a finite-horizon Markov Decision Process (MDP), denoted by $\mathcal{M} = (\mathcal{S}, \mathcal{A}, \mathcal{P}, \mathcal{R}, \gamma, H)$. The policy $\pi_\theta(a_t|s_t)$ maps states s_t (RGB images and proprioception) to actions a_t . The environment transitions according to $\mathcal{P}(s_{t+1}|s_t, a_t)$ and provides a reward $r_t = \mathcal{R}(s_t, a_t)$. The goal is to maximize the expected discounted return $J(\pi) = \mathbb{E}_\pi[\sum_{t=0}^H \gamma^t r_t]$. We use expert demonstrations \mathcal{D}_E as references for policy deviation.

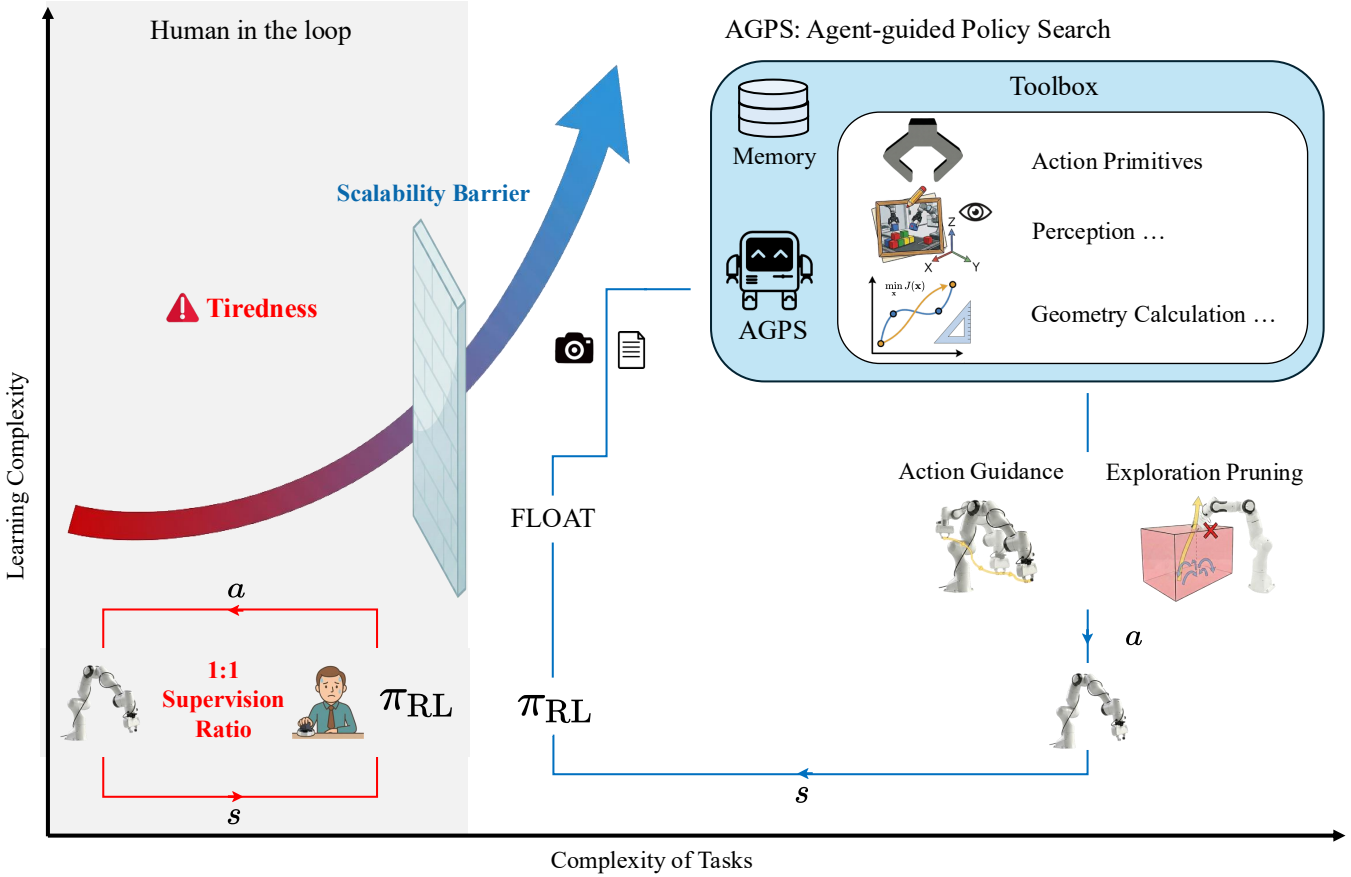


Fig. 1: **Overview** Left: HIL methods encounter a scalability barrier as task complexity rises, restricted by the 1:1 supervision ratio and operator fatigue. Right: AGPS transcends this barrier by automating supervision. The system employs FLOAT as an asynchronous trigger to monitor policy performance. When a deviation is detected, the agent recalls memory and leverages a toolbox (Action Primitives, Perception, Geometry) for spatial reasoning. These interventions manifest as Action Guidance for trajectory correction and Exploration Pruning for spatial constraining.

B. Optimal Transport for Trajectory Matching

We use OT as a metric to quantify how current policy rollouts deviate from expert behaviors. OT provides a geometric distance between distributions that is resilient to temporal shifts. We map observations from expert trajectories \mathcal{T}_e and agent rollouts \mathcal{T}_b into a latent space using a pretrained encoder $\phi(\cdot)$, yielding embeddings X_e and X_b . The OT distance $d_{\text{OT}}(X_e, X_b)$ is the minimum cost to transport mass between these distributions:

$$d_{\text{OT}}(X_e, X_b) = \min_{\mu} \sum_{i,j} C_{ij} \mu_{ij}$$

subject to marginal constraints $\sum_j \mu_{ij} = \frac{1}{L_e}$ and $\sum_i \mu_{ij} = \frac{1}{L_b}$. The cost matrix $C_{ij} = 1 - \cos(\phi(o_{e,i}), \phi(o_{b,j}))$ measures embedding dissimilarity. This defines the FLOAT Index, $\lambda(\mathcal{T}_b) = \min_n d_{\text{OT}}(\phi(\mathcal{T}_e^n), \phi(\mathcal{T}_b))$, measuring the deviation from expert manifolds.

III. AGENT-GUIDED POLICY SEARCH

We propose Agent-guided Policy Search (AGPS). As illustrated in Figure 1, the framework consists of two core com-

ponents: the asynchronous failure detector (FLOAT) which monitors the policy π_{RL} , and a toolbox that translates semantic understanding into actionable geometric constraints. The pseudocode is in Appendix B.

A. Asynchronous Failure Detection (FLOAT)

The multimodal agents have high inference latency, making them unsuitable for high-frequency robotic control. To mitigate the high inference latency associated with agents, we employ FLOAT as a real-time trigger. This module monitors policy execution and solicits guidance only when a significant deviation from the expert distribution is detected.

We utilize a pre-trained visual encoder $\phi(\cdot)$ (DINOv2 ViT-B/14 [35]) to project observations into a latent feature space. At timestep t , the system calculates a deviation score λ_t based on the OT distance between the current rollout \mathcal{T}_b and the set of expert demonstrations \mathcal{T}_e :

$$\lambda_t = \min_{n \in 1, \dots, N} d_{\text{OT}}(\phi(\mathcal{T}_e^n), \phi(\mathcal{T}_b, 1:t)) \quad (1)$$

The system follows a thresholding protocol where Λ is set to the 95th percentile of FLOAT indices from successful

transitions in the replay buffer.

- Autonomous Exploration ($\lambda_t \leq \Lambda$): The policy π_{RL} continues execution to maintain high interaction throughput.
- Agent Intervention ($\lambda_t > \Lambda$): The system pauses and invokes the Agent to provide corrective guidance.

B. The toolbox

The primary challenge in this pipeline is grounding abstract semantic knowledge in physical world. We address this by developing a toolbox of executable modules that allow the agent to reason about the workspace with geometric precision.

1) *Perception Module*: The agent utilizes a VLM (Qwen3-VL [4]) to identify task-relevant keypoints (e.g., "USB port") from RGBD images. The VLM outputs 2D pixel coordinates \mathbf{u}_{key} , which are then deprojected into 3D world coordinates P_{world} by Eq. 2,

$$P_{world} = R^{-1} (D(\mathbf{u}_{key}) \cdot K^{-1}[\mathbf{u}_{key}, 1]^T - \mathbf{t}) \quad (2)$$

where $K \in \mathbb{R}^{3 \times 3}$ is the camera intrinsic matrix, and $[R, \mathbf{t}] \in SE(3)$ represents the camera extrinsic parameters relative to the robot base. This transformation maps semantic features from the image plane into the robot's task space, providing a metric foundation for geometric guidance.

2) *Action Primitives Library*: We define a library of atomic Action Primitives to serve as waypoint generators. Based on the current TCP pose and gripper state, these primitives calculate specific target configurations. They include discrete actions (e.g., Grasp, Release) and continuous motions (e.g., MoveDelta, Lift). This modular design allows the agent to compose precise geometric interventions efficiently.

3) *Memory Module*: To reduce system latency, an episodic memory module caches mappings between subgoals and spatial constraints, such as bounding boxes \mathcal{C}_{box} . Before invoking the VLM, the system queries this memory; if a historical rollout was successful, the agent reuses the stored bounding box to avoid redundant VLM inference.

C. Automated Guidance Mechanisms

Leveraging the toolbox, AGPS provides two types of interventions:

1) *Action Guidance*: Upon a FLOAT trigger, the agent identifies the failure mode and synthesizes a corrective trajectory. By selecting appropriate action primitives and grounding them through the Geometry Module, the agent generates precise corrective waypoints. This mechanism provides a stable supervision signal that helps the policy not stray too far from the expert distribution.

2) *Exploration Pruning*: The agent prunes irrelevant exploration to accelerate learning. The agent defines a 3D bounding box \mathcal{C}_{box} that encapsulates the task-relevant volume. During RL training, any action leading outside this volume is masked. By constraining the search space to a semantically valid manifold, AGPS prevents the robot from wasting samples in task-irrelevant regions.

IV. EXPERIMENTS

Our experiments aim to address four questions: (1) Can AGPS significantly improve sample efficiency (Section IV-C)? (2) Does the frequency of agent interventions decay as the policy improves (Section IV-D)? (3) What is the quality of AGPS's intervention (Section IV-E)? (4) Does memory accelerate training (Section IV-F)?

A. Experimental Setup

We evaluate AGPS on two tasks: USB Insertion (high-precision rigid assembly) and Chinese Knot Hanging (deformable object manipulation). The experimental workspaces are illustrated in Figure 7. Details are in Appendix C.

- **USB Insertion**: Align and insert a USB connector into a tight port.
- **Chinese Knot Hanging**: Hang a Chinese knot onto a hook.

B. Baselines and Metrics

We compare AGPS with three baselines: SERL (off-policy RL with offline demonstrations), HIL-SERL (SERL with human interventions), and VLM Planner (open-loop primitives without RL). All methods use identical network architectures and hyperparameters to ensure consistency.

The performance is measured by three metrics. Success Rate tracks completion probability over 10 randomized trials, while Time to Convergence records the wall-clock time to reach 100% success. Intervention Ratio measures the frequency of external guidance or agent activations per episode.

C. Overall performance comparison

AGPS shows superior sample efficiency in the USB task (Figure 2, left). It reaches 40% success at Step 400 and 100% by Step 600 (8 minutes), outperforming HIL-SERL. This gain stems from Exploration Pruning. As shown in Figure 3b, AGPS restricts the gripper to a task-relevant bounding box, preventing wasted exploration. SERL fails (0%) due to the vast search space. The VLM planner also fails (0%) because its open-loop keypoints prediction lack the sub-millimeter precision needed for insertion, proving that closed-loop control is essential.

In the Chinese Knot task (Figure 2, right), AGPS converges significantly faster than HIL-SERL. HIL-SERL remains at 0% success rate until Step 3,000, hampered by inconsistent human interventions common in deformable object manipulation. In contrast, AGPS reaches 90% success by Step 3,000 (42 min) and 100% by Step 4,000. This confirms that consistent agent-generated waypoints provide more effective guidance than high-variance human teleoperation. The VLM baseline achieves 90% success by localizing the hook but occasionally fails due to perception noise. AGPS closes this gap by using VLM outputs as coarse constraints and RL to manage local deformations, and SERL remains at 0%.

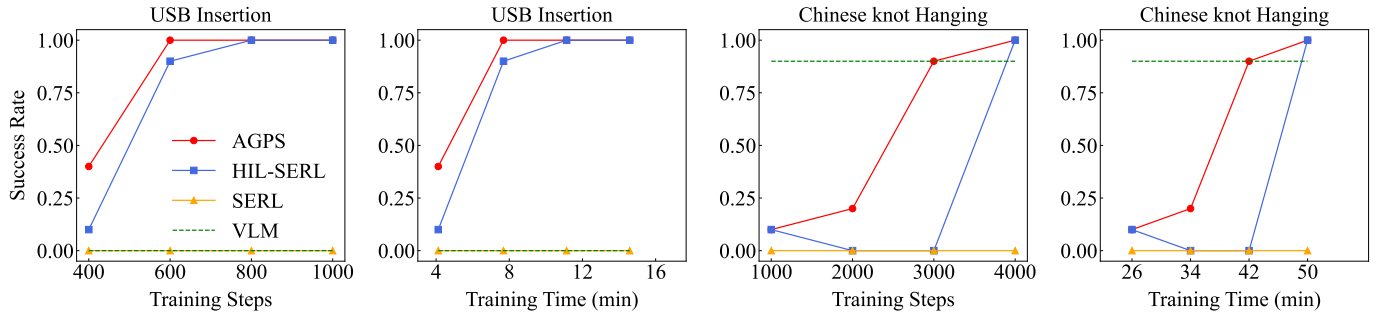
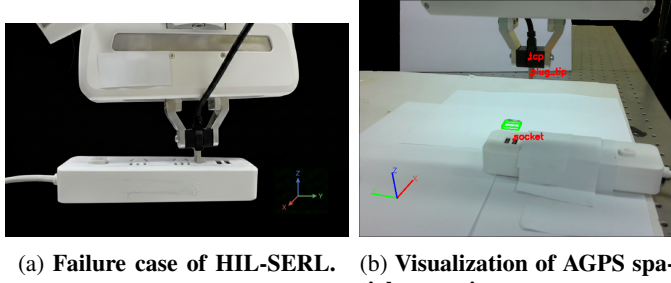


Fig. 2: **Overall performance comparisons.** The curves illustrate the evolution of success rate with respect to training steps and wall-clock time. We evaluate the policy at 4 distinct checkpoints, with success rates calculated over 10 evaluation episodes per checkpoint.



(a) Failure case of HIL-SERL. (b) Visualization of AGPS spatial reasoning.

Fig. 3: Comparison of USB insertion tasks. (a) illustrates a failure case; (b) shows the AGPS spatial reasoning where red points denote semantic keypoints and the green box represents the task-relevant volume for exploration pruning.

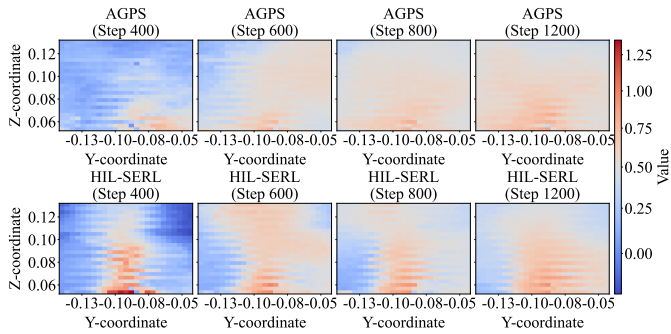


Fig. 4: **Visualization of policy training dynamics.** The heatmaps visualize the value distribution across the Y-Z spatial coordinates at different training steps (400 to 1200). (Bottom) HIL-SERL learns a narrow high-value corridor. This indicates overfitting to specific human demonstrations, leaving surrounding states with near-zero value (blue regions). (Top) AGPS develops a broad high-value funnel. This shows the policy has learned recovery behaviors for states deviating from the optimal trajectory, enabling it to handle misalignments.

D. Intervention Frequency

We tracked the number of VLM triggers during training (Figure 5, Right). In the USB Insertion (Red) task, the intervention rate peaks early. It drops to 0 by Rollout 45. The

policy π_{RL} quickly masters the insertion. In the Chinese Knot (Blue) task, guidance starts at the maximum (10 triggers). It decreases slowly due to complex rope dynamics. Interventions reach near zero around Rollout 100. This decline shows that π_{RL} progressively aligns with the success distribution, keeping deviation scores below the FLOAT threshold. The policy has internalized the guidance and achieved independent mastery.

E. Generalization and Q-value Analysis

We analyze the learned Q-value landscapes to investigate how exploration strategies affect policy generalization (Figure 4). HIL-SERL (bottom row) forms a narrow high-value corridor because human operators demonstrate only the most direct paths. This bias causes the policy to overfit to a thin trajectory, leaving off-center states with near-zero values (blue regions). Conversely, AGPS (top row) develops a broader high-value landscape. Since the FLOAT trigger only intervenes during critical failures, the policy autonomously resolves minor misalignments, forcing it to learn recovery behaviors. This value distribution directly impacts physical performance. In a test case (Figure 3a), HIL-SERL consistently fails. Lacking gradient information in this low-value region ($Y \approx -0.13$), the robot freezes or drifts. AGPS succeeds because its broad landscape covers that state, providing the necessary gradients to execute corrective shifts toward the slot. This confirms that agent-guided exploration enables the policy to recover from diverse initial states without human intervention.

F. Memory accelerates training

We conducted an ablation study on the USB task to evaluate the memory module (Figure 5, left). AGPS with Memory (Red) converges by Step 800, achieving a 2 \times speedup over the version without memory (Blue), which requires 1600 steps. This acceleration results from reusing validated spatial constraints. By retrieving successful bounding boxes from history, the system bypasses redundant VLM computations. Consequently, the policy converges significantly faster by avoiding repeated calls to the agent.

V. DISCUSSION: AGPS AS A SEMANTIC WORLD MODEL

Real-world reinforcement learning is limited by expensive, serial interactions. Our results suggest that multimodal agents

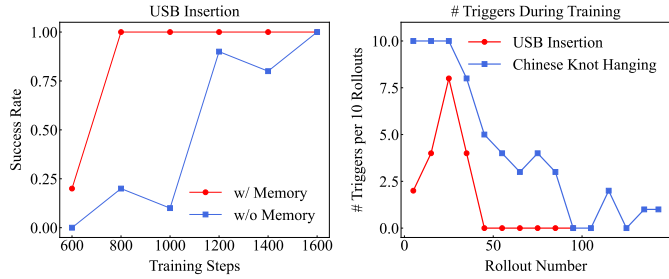


Fig. 5: **Ablation and intervention analysis.** (Left.) The memory module (red) accelerates convergence by 2 \times compared to the baseline (blue). (Right.) The number of triggers per 10 rollouts decreases over time. Both tasks achieve zero intervention ultimately.

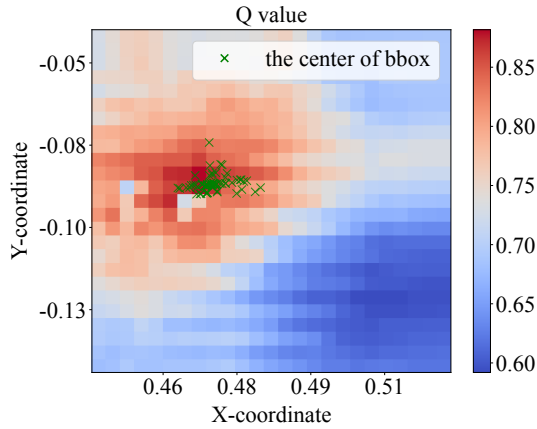


Fig. 6: **Visualization of spatial alignment.** The heatmap displays the learned Q-value distribution of the converged HIL-SERL policy, where red indicates high value. Green crosses mark the centers of bounding boxes generated zero-shot by the Agent. Their tight alignment with the high-value region confirms that the agent's semantic priors accurately predict the high Q-value region without prior training.

can be viewed as semantic world models to address this bottleneck. This is evidenced by the spatial alignment shown in Figure 6. The heatmap displays the learned Q-value landscape of HIL-SERL. Green crosses, marking zero-shot bounding box centers generated by our agent, align closely with the high Q-value regions (red).

While the baseline requires human intervention to find the high Q-value region, the agent identifies it immediately through semantic reasoning. This suggests that foundation models possess an intrinsic value prior, predicting the high-value region without interaction. By using this prior to prune the exploration space, AGPS allows the RL algorithm to focus on task-relevant regions. This approach replaces human supervision with autonomous semantic constraints, enabling more scalable real-world learning.

VI. LIMITATIONS

Our framework faces limitations primarily regarding the foundation model. First, the system's performance ceiling is constrained by the VLM's visual grounding capability, instances of hallucination or imprecise localization under occlusion can lead to task failure. Second, the inference latency of large-scale models remains a bottleneck. High computational costs limit the frequency of guidance, which restricts the system's applicability in highly dynamic scenarios requiring high-frequency feedback.

VII. CONCLUSION

In this work, we introduced Agent-guided Policy Search (AGPS). This framework automates real-world reinforcement learning by replacing human supervision with a multimodal agent. By integrating asynchronous failure detection with an executable toolbox, the system grounds high-level semantic reasoning into precise physical constraints. Real-world experiments on rigid and deformable object manipulation demonstrate that AGPS outperforms the sample efficiency of HIL methods. Crucially, it achieves this with zero human intervention. Our analysis further reveals that the agent can be viewed as a pre-trained semantic world model. It aligns exploration with high-value task manifolds through zero-shot spatial pruning. These findings suggest a fundamental shift for real-world robotic learning. The path to scalability lies in leveraging agents to structure physical exploration, effectively replacing unscalable human labor with robust, autonomous semantic priors.

REFERENCES

- [1] Michael Ahn, Anthony Brohan, Noah Brown, Yevgen Chebotar, Omar Cortes, Byron David, Chelsea Finn, Chuyuan Fu, Keerthana Gopalakrishnan, Karol Hausman, et al. Do as i can, not as i say: Grounding language in robotic affordances. *arXiv preprint arXiv:2204.01691*, 2022.
- [2] Michael Ahn, Debidatta Dwibedi, Chelsea Finn, Montserrat Gonzalez Arenas, Keerthana Gopalakrishnan, Karol Hausman, brian ichter, Alex Irpan, Nikhil J Joshi, Ryan Julian, Sean Kirmani, Isabel Leal, Tsang-Wei Edward Lee, Sergey Levine, Yao Lu, sharath maddineni, Kanishka Rao, Dorsa Sadigh, Pannag R Sanketi, Pierre Sermanet, Quan Vuong, Stefan Welker, Fei Xia, Ted Xiao, Peng Xu, Sichun Xu, and Zhusuo Xu. AutORT: Embodied foundation models for large scale orchestration of robotic agents. In *First Workshop on Vision-Language Models for Navigation and Manipulation at ICRA 2024*, 2024. URL <https://openreview.net/forum?id=DYcCveNeR1>.
- [3] Lars Ankine, Zhenyu Jiang, Rocky Duan, Guanya Shi, Pieter Abbeel, and Anusha Nagabandi. Residual off-policy rl for finetuning behavior cloning policies. *arXiv preprint arXiv:2509.19301*, 2025.
- [4] Shuai Bai, Yuxuan Cai, Ruizhe Chen, Keqin Chen, Xionghui Chen, Zesen Cheng, Lianghao Deng, Wei Ding,

Chang Gao, Chunjiang Ge, Wenbin Ge, Zhifang Guo, Qidong Huang, Jie Huang, Fei Huang, Binyuan Hui, Shutong Jiang, Zhaohai Li, Mingsheng Li, Mei Li, Kaixin Li, Zicheng Lin, Junyang Lin, Xuejing Liu, Jiawei Liu, Chenglong Liu, Yang Liu, Dayiheng Liu, Shixuan Liu, Dunjie Lu, Ruilin Luo, Chenxu Lv, Rui Men, Lingchen Meng, Xuancheng Ren, Xingzhang Ren, Sibo Song, Yuchong Sun, Jun Tang, Jianhong Tu, Jianqiang Wan, Peng Wang, Pengfei Wang, Qiuyue Wang, Yuxuan Wang, Tianbao Xie, Yiheng Xu, Haiyang Xu, Jin Xu, Zhibo Yang, Mingkun Yang, Jianxin Yang, An Yang, Bowen Yu, Fei Zhang, Hang Zhang, Xi Zhang, Bo Zheng, Humen Zhong, Jingren Zhou, Fan Zhou, Jing Zhou, Yuanzhi Zhu, and Ke Zhu. Qwen3-vl technical report. *arXiv preprint arXiv:2511.21631*, 2025.

[5] Philip J Ball, Laura Smith, Ilya Kostrikov, and Sergey Levine. Efficient online reinforcement learning with offline data. In *International Conference on Machine Learning*, pages 1577–1594. PMLR, 2023.

[6] Philip J. Ball, Laura Smith, Ilya Kostrikov, and Sergey Levine. Efficient online reinforcement learning with offline data. In Andreas Krause, Emma Brunskill, Kyunghyun Cho, Barbara Engelhardt, Sivan Sabato, and Jonathan Scarlett, editors, *Proceedings of the 40th International Conference on Machine Learning*, volume 202 of *Proceedings of Machine Learning Research*, pages 1577–1594. PMLR, 23–29 Jul 2023. URL <https://proceedings.mlr.press/v202/ball23a.html>.

[7] Anthony Brohan, Noah Brown, Justice Carbajal, Yevgen Chebotar, Joseph Dabis, Chelsea Finn, Keerthana Gopalakrishnan, Karol Hausman, Alex Herzog, Jasmine Hsu, et al. Rt-1: Robotics transformer for real-world control at scale. *arXiv preprint arXiv:2212.06817*, 2022.

[8] Boyuan Chen, Zhuo Xu, Sean Kirmani, Brian Ichter, Dorsa Sadigh, Leonidas Guibas, and Fei Xia. Spatialvlm: Endowing vision-language models with spatial reasoning capabilities. In *Proceedings of the IEEE/CVF Conference on Computer Vision and Pattern Recognition (CVPR)*, pages 14455–14465, June 2024.

[9] Yuhui Chen, Shuai Tian, Shugao Liu, Yingting Zhou, Haoran Li, and Dongbin Zhao. Conrft: A reinforced fine-tuning method for vla models via consistency policy. In *Proceedings of Robotics: Science and Systems, RSS 2025, Los Angeles, CA, USA, Jun 21-25, 2025*. doi: 10.15607/RSS.2025.XXI.019.

[10] Perry Dong, Qiyang Li, Dorsa Sadigh, and Chelsea Finn. Expo: Stable reinforcement learning with expressive policies. *arXiv preprint arXiv:2507.07986*, 2025.

[11] Danny Driess, Fei Xia, Mehdi SM Sajjadi, Corey Lynch, Aakanksha Chowdhery, Ayzaan Wahid, Jonathan Tompson, Quan Vuong, Tianhe Yu, Wenlong Huang, et al. Palm-e: An embodied multimodal language model. 2023.

[12] Yilun Du, Sherry Yang, Bo Dai, Hanjun Dai, Ofir Nachum, Josh Tenenbaum, Dale Schuurmans, and Pieter Abbeel. Learning universal policies via text-guided video generation. In A. Oh, T. Naumann, A. Globerson, K. Saenko, M. Hardt, and S. Levine, editors, *Advances in Neural Information Processing Systems*, volume 36, pages 9156–9172. Curran Associates, Inc., 2023. URL https://proceedings.neurips.cc/paper_files/paper/2023/file/1d5b9233ad716a43be5c0d3023cb82d0-Paper-Conference.pdf.

[13] Jiafei Duan, Wentao Yuan, Wilbert Pumacay, Yi Ru Wang, Kiana Ehsani, Dieter Fox, and Ranjay Krishna. Manipulate-anything: Automating real-world robots using vision-language models. In *Conference on Robot Learning*, pages 5326–5350. PMLR, 2025.

[14] Gabriel Dulac-Arnold, Daniel Mankowitz, and Todd Hester. Challenges of real-world reinforcement learning. *arXiv preprint arXiv:1904.12901*, 2019.

[15] Linxi Fan, Guanzhi Wang, Yunfan Jiang, Ajay Mandlekar, Yuncong Yang, Haoyi Zhu, Andrew Tang, De-An Huang, Yuke Zhu, and Anima Anandkumar. Minedojo: Building open-ended embodied agents with internet-scale knowledge. In S. Koyejo, S. Mohamed, A. Agarwal, D. Belgrave, K. Cho, and A. Oh, editors, *Advances in Neural Information Processing Systems*, volume 35, pages 18343–18362. Curran Associates, Inc., 2022. URL https://proceedings.neurips.cc/paper_files/paper/2022/file/74a67268c5cc5910f64938cac4526a90-Paper-Datasets_and_Benchmarks.pdf.

[16] Ankit Goyal, Valts Blukis, Jie Xu, Yijie Guo, Yu-Wei Chao, and Dieter Fox. RVT-2: Learning precise manipulation from few demonstrations. In *RSS 2024 Workshop: Data Generation for Robotics*, 2024. URL <https://openreview.net/forum?id=TAGsz6OQKE>.

[17] Huy Ha, Pete Florence, and Shuran Song. Scaling up and distilling down: Language-guided robot skill acquisition. In *Conference on Robot Learning*, pages 3766–3777. PMLR, 2023.

[18] Joy Hsu, Jiayuan Mao, and Jiajun Wu. Ns3d: Neuro-symbolic grounding of 3d objects and relations. In *Proceedings of the IEEE/CVF Conference on Computer Vision and Pattern Recognition (CVPR)*, pages 2614–2623, June 2023.

[19] Hengyuan Hu, Suvir Mirchandani, and Dorsa Sadigh. Imitation bootstrapped reinforcement learning. *arXiv preprint arXiv:2311.02198*, 2023.

[20] Wenlong Huang, Chen Wang, Ruohan Zhang, Yunzhu Li, Jiajun Wu, and Li Fei-Fei. Voxposer: Composable 3d value maps for robotic manipulation with language models. *arXiv preprint arXiv:2307.05973*, 2023.

[21] Wenlong Huang, Fei Xia, Ted Xiao, Harris Chan, Jacky Liang, Pete Florence, Andy Zeng, Jonathan Tompson, Igor Mordatch, Yevgen Chebotar, Pierre Sermanet, Tomas Jackson, Noah Brown, Linda Luu, Sergey Levine, Karol Hausman, and brian ichter. Inner monologue: Embodied reasoning through planning with language models. In Karen Liu, Dana Kulic, and Jeff Ichnowski, editors, *Proceedings of The 6th Conference on Robot Learn-*

ing, volume 205 of *Proceedings of Machine Learning Research*, pages 1769–1782. PMLR, 14–18 Dec 2023. URL <https://proceedings.mlr.press/v205/huang23c.html>.

[22] Wenlong Huang, Chen Wang, Yunzhu Li, Ruohan Zhang, and Fei-Fei Li. Rekep: Spatio-temporal reasoning of relational keypoint constraints for robotic manipulation. In Pulkit Agrawal, Oliver Kroemer, and Wolfram Burgard, editors, *Proceedings of The 8th Conference on Robot Learning*, volume 270 of *Proceedings of Machine Learning Research*, pages 4573–4602. PMLR, 06–09 Nov 2024. URL <https://proceedings.mlr.press/v270/huang25g.html>.

[23] Yunfan Jiang, Agrim Gupta, Zichen Zhang, Guanzhi Wang, Yongqiang Dou, Yanjun Chen, Li Fei-Fei, Anima Anandkumar, Yuke Zhu, and Linxi Fan. VIMA: General robot manipulation with multimodal prompts. In *NeurIPS 2022 Foundation Models for Decision Making Workshop*, 2022. URL <https://openreview.net/forum?id=oU2DzdTI94>.

[24] Tobias Johannink, Shikhar Bahl, Ashvin Nair, Jianlan Luo, Avinash Kumar, Matthias Loskyll, Juan Aparicio Ojea, Eugen Solowjow, and Sergey Levine. Residual reinforcement learning for robot control. In *2019 international conference on robotics and automation (ICRA)*, pages 6023–6029. IEEE, 2019.

[25] Sergey Levine and Vladlen Koltun. Guided policy search. In *International conference on machine learning*, pages 1–9. PMLR, 2013.

[26] Jacky Liang, Wenlong Huang, Fei Xia, Peng Xu, Karol Hausman, Brian Ichter, Pete Florence, and Andy Zeng. Code as policies: Language model programs for embodied control. In *2023 IEEE International Conference on Robotics and Automation (ICRA)*, pages 9493–9500, 2023. doi: 10.1109/ICRA48891.2023.10160591.

[27] Fangchen Liu, Kuan Fang, Pieter Abbeel, and Sergey Levine. MOKA: Open-vocabulary robotic manipulation through mark-based visual prompting. In *First Workshop on Vision-Language Models for Navigation and Manipulation at ICRA 2024*, 2024. URL <https://openreview.net/forum?id=K8eoYUofbQ>.

[28] Jianlan Luo, Zheyuan Hu, Charles Xu, You Liang Tan, Jacob Berg, Archit Sharma, Stefan Schaal, Chelsea Finn, Abhishek Gupta, and Sergey Levine. Serl: A software suite for sample-efficient robotic reinforcement learning. In *2024 IEEE International Conference on Robotics and Automation (ICRA)*, pages 16961–16969. IEEE, 2024.

[29] Jianlan Luo, Charles Xu, Jeffrey Wu, and Sergey Levine. Precise and dexterous robotic manipulation via human-in-the-loop reinforcement learning. *Science Robotics*, 10(105):eads5033, 2025.

[30] Yecheng Jason Ma, Shagun Sodhani, Dinesh Jayaraman, Osbert Bastani, Vikash Kumar, and Amy Zhang. VIP: Towards universal visual reward and representation via value-implicit pre-training. In *The Eleventh International Conference on Learning Representations*, 2023. URL <https://openreview.net/forum?id=YJ7o2wetJ2>.

[31] Yecheng Jason Ma, William Liang, Guanzhi Wang, De-An Huang, Osbert Bastani, Dinesh Jayaraman, Yuke Zhu, Linxi Fan, and Anima Anandkumar. Eureka: Human-level reward design via coding large language models. In *The Twelfth International Conference on Learning Representations*, 2024. URL <https://openreview.net/forum?id=IEduRUO55F>.

[32] Ashvin Nair, Abhishek Gupta, Murtaza Dalal, and Sergey Levine. Awac: Accelerating online reinforcement learning with offline datasets. *arXiv preprint arXiv:2006.09359*, 2020.

[33] Suraj Nair, Aravind Rajeswaran, Vikash Kumar, Chelsea Finn, and Abhinav Gupta. R3m: A universal visual representation for robot manipulation. In Karen Liu, Dana Kulic, and Jeff Ichnowski, editors, *Proceedings of The 6th Conference on Robot Learning*, volume 205 of *Proceedings of Machine Learning Research*, pages 892–909. PMLR, 14–18 Dec 2023. URL <https://proceedings.mlr.press/v205/nair23a.html>.

[34] Mitsuhiro Nakamoto, Simon Zhai, Anikait Singh, Max Sobol Mark, Yi Ma, Chelsea Finn, Aviral Kumar, and Sergey Levine. Cal-ql: Calibrated offline rl pre-training for efficient online fine-tuning. *Advances in Neural Information Processing Systems*, 36:62244–62269, 2023.

[35] Maxime Oquab, Timothée Darcet, Théo Moutakanni, Huy V Vo, Marc Szafraniec, Vasil Khalidov, Pierre Fernandez, Daniel HAZIZA, Francisco Massa, Alaaeldin El-Nouby, et al. Dinov2: Learning robust visual features without supervision. *Transactions on Machine Learning Research*.

[36] Gabriel Peyré, Marco Cuturi, et al. Computational optimal transport: With applications to data science. *Foundations and Trends® in Machine Learning*, 11(5–6):355–607, 2019.

[37] Aravind Rajeswaran, Vikash Kumar, Abhishek Gupta, Giulia Vezzani, John Schulman, Emanuel Todorov, and Sergey Levine. Learning complex dexterous manipulation with deep reinforcement learning and demonstrations. *arXiv preprint arXiv:1709.10087*, 2017.

[38] Mohit Shridhar, Lucas Manuelli, and Dieter Fox. Cliport: What and where pathways for robotic manipulation. In Aleksandra Faust, David Hsu, and Gerhard Neumann, editors, *Proceedings of the 5th Conference on Robot Learning*, volume 164 of *Proceedings of Machine Learning Research*, pages 894–906. PMLR, 08–11 Nov 2022. URL <https://proceedings.mlr.press/v164/shridhar22a.html>.

[39] Mohit Shridhar, Lucas Manuelli, and Dieter Fox. Perceiver-actor: A multi-task transformer for robotic manipulation. In Karen Liu, Dana Kulic, and Jeff Ichnowski, editors, *Proceedings of The 6th Conference on Robot Learning*, volume 205 of *Proceedings of Machine Learning Research*, pages 785–799. PMLR, 14–18 Dec 2023. URL <https://proceedings.mlr.press/v205/shridhar23a.html>.

[40] Ishika Singh, Valts Blukis, Arsalan Mousavian, Ankit Goyal, Danfei Xu, Jonathan Tremblay, Dieter Fox, Jesse

Thomason, and Animesh Garg. Progprompt: Generating situated robot task plans using large language models. In *Workshop on Language and Robotics at CoRL 2022*, 2022. URL https://openreview.net/forum?id=3K4-U_5cRw.

[41] Richard S Sutton, Andrew G Barto, et al. *Introduction to reinforcement learning*, volume 135. MIT press Cambridge, 1998.

[42] Ikechukwu Uchendu, Ted Xiao, Yao Lu, Banghua Zhu, Mengyuan Yan, Joséphine Simon, Matthew Bennice, Chuyuan Fu, Cong Ma, Jiantao Jiao, et al. Jump-start reinforcement learning. In *International Conference on Machine Learning*, pages 34556–34583. PMLR, 2023.

[43] Andrés Villa, Juan León Alcázar, Motasem Alfarra, Kumat Alhamoud, Julio Hurtado, Fabian Caba Heilbron, Alvaro Soto, and Bernard Ghanem. Pivot: Prompting for video continual learning. In *Proceedings of the IEEE/CVF Conference on Computer Vision and Pattern Recognition*, pages 24214–24223, 2023.

[44] Guanzhi Wang, Yuqi Xie, Yunfan Jiang, Ajay Mandlekar, Chaowei Xiao, Yuke Zhu, Linxi Fan, and Anima Anandkumar. Voyager: An open-ended embodied agent with large language models. *Transactions on Machine Learning Research*, 2024. ISSN 2835-8856. URL <https://openreview.net/forum?id=ehfRiF0R3a>.

[45] Wenli Xiao, Haotian Lin, Andy Peng, Haoru Xue, Tairan He, Yuqi Xie, Fengyuan Hu, Jimmy Wu, Zhengyi Luo, Linxi Fan, et al. Self-improving vision-language-action models with data generation via residual rl. *arXiv preprint arXiv:2511.00091*, 2025.

[46] Tianbao Xie, Siheng Zhao, Chen Henry Wu, Yitao Liu, Qian Luo, Victor Zhong, Yanchao Yang, and Tao Yu. Text2reward: Reward shaping with language models for reinforcement learning. In *The Twelfth International Conference on Learning Representations*, 2024. URL <https://openreview.net/forum?id=tUM39YTRxH>.

[47] Weirui Ye, Yunsheng Zhang, Haoyang Weng, Xianfan Gu, Shengjie Wang, Tong Zhang, Mengchen Wang, Pieter Abbeel, and Yang Gao. Reinforcement learning with foundation priors: Let embodied agent efficiently learn on its own. In Pulkit Agrawal, Oliver Kroemer, and Wolfram Burgard, editors, *Proceedings of The 8th Conference on Robot Learning*, volume 270 of *Proceedings of Machine Learning Research*, pages 185–208. PMLR, 06–09 Nov 2025. URL <https://proceedings.mlr.press/v270/ye25a.html>.

[48] Wenhao Yu, Nimrod Gileadi, Chuyuan Fu, Sean Kirmani, Kuang-Huei Lee, Montse Gonzalez Arenas, Hao-Tien Lewis Chiang, Tom Erez, Leonard Hasenclever, Jan Humplik, et al. Language to rewards for robotic skill synthesis. *arXiv preprint arXiv:2306.08647*, 2023.

[49] Wenye Yu, Jun Lv, Zixi Ying, Yang Jin, Chuan Wen, and Cewu Lu. Armada: Autonomous online failure detection and human shared control empower scalable real-world deployment and adaptation. *arXiv preprint arXiv:2510.02298*, 2025.

[50] Wentao Yuan, Jiafei Duan, Valts Blukis, Wilbert Pumacay, Ranjay Krishna, Adithyavairavan Murali, Arsalan Mousavian, and Dieter Fox. Robopoint: A vision-language model for spatial affordance prediction in robotics. In Pulkit Agrawal, Oliver Kroemer, and Wolfram Burgard, editors, *Proceedings of The 8th Conference on Robot Learning*, volume 270 of *Proceedings of Machine Learning Research*, pages 4005–4020. PMLR, 06–09 Nov 2025. URL <https://proceedings.mlr.press/v270/yuan25c.html>.

[51] Xiu Yuan, Tongzhou Mu, Stone Tao, Yunhao Fang, Mengke Zhang, and Hao Su. Policy decorator: Model-agnostic online refinement for large policy model. *arXiv preprint arXiv:2412.13630*, 2024.

[52] Brianna Zitkovich, Tianhe Yu, Sichun Xu, Peng Xu, Ted Xiao, Fei Xia, Jialin Wu, Paul Wohlhart, Stefan Welker, Ayaan Wahid, et al. Rt-2: Vision-language-action models transfer web knowledge to robotic control. In *Conference on Robot Learning*, pages 2165–2183. PMLR, 2023.

APPENDIX

A. Related Work

Real-world RL. Improving the sample efficiency of real-world robotic reinforcement learning (RL) has involved several key strategies: developing highly efficient off-policy algorithms [5, 28]; leveraging demonstrations and prior data through hybrid methods [37, 32, 19, 34], or guided curricula [42]; employing residual learning architectures [24, 3, 51, 10, 45] to refine base policies. To further accelerate exploration, Human-in-the-Loop (HIL) methods like HIL-SERL [29] and ConRFT [9] leverage online human corrections to prune the search space and ensure safety, akin to the constrained trajectory optimization in GPS [25]. However, HIL approaches are bounded by a strict 1:1 supervision ratio. In contrast, our work replaces human oversight with a multimodal agent, providing deterministic, kinematically consistent supervision that scales infinitely without human intervention.

Foundation models for policy learning. Foundational models are transforming robotic policy learning across multiple paradigms. Early works like SayCan [1] and Inner Monologue [21] used Large Language Models(LLMs) for semantic planning, later extended by Code as Policies [26], ProgPrompt [40], and VoxPoser [20] for program synthesis. For direct perception-to-action mapping, RT-1[7], RT-2[52], PaLM-E [11], VIMA [23], and MineDojo [15] demonstrated large-scale visuomotor control. To automate reward design, Eureka [31], L2R [48], and ReKep [22] leverage LLMs or Vision Language Models(VLMs) to generate reward functions or cost constraints. Foundation Models also provide priors for RL, as in RLFP[47], and scale data via automated demonstration generation for policies [13, 17, 39, 16]. Visual grounding is advanced MOKA [27], PIVOT [43], and Robopoint [50], while spatial reasoning is studied in NS3D [18] and SpatialVLM [8]. Additional contributions include visual priors [30, 33],

Algorithm 1 Agent-guided Policy Search (AGPS)

Require: Pre-trained VLM Agent \mathcal{A}_{vlm} , Policy π_θ , Critic Q_ϕ .
 Expert dataset \mathcal{D}_E . Batch size B .

- 1: Initialize online buffer $\mathcal{R} \leftarrow \emptyset$, Episodic Memory $\mathcal{M} \leftarrow \emptyset$.
- 2: Compute failure threshold Λ based on \mathcal{D} .
- 3: Randomly initialize π_θ and Q_ϕ .
- 4: **# Start Policy Learning Thread:**
- 5: **Wait until** \mathcal{R} contains at least 100 transitions.
- 6: **for** each training step **do**
- 7: Sample batch $b_{\text{demo}} \in \mathcal{D}_E$ and $b_{\text{online}} \in \mathcal{R}$.
- 8: Update θ, ϕ using $b_{\text{demo}} \cup b_{\text{online}}$.
- 9: **end for**
- 10: **# Start Interaction Thread:**
- 11: **for** each interaction step t **do**
- 12: Compute deviation $\lambda_t \leftarrow \text{FLOAT}(s_t, \mathcal{D}_E)$.
- 13: **if** $\lambda_t \leq \Lambda$ **then**
- 14: Sample action $a_t \sim \pi_\theta(\cdot | s_t)$.
- 15: **else**
- 16: **# Agent Intervention**
- 17: Extract sub goal c_t from s_t .
- 18: $\mu \leftarrow \mathcal{A}_{\text{vlm}}.\text{DecideMode}(s_t, c_t)$.
- 19: **if** μ is **Exploration Pruning** **then**
- 20: $\text{flag} \leftarrow \mathcal{A}_{\text{vlm}}.\text{CheckMemory}(c_t, \mathcal{M})$.
- 21: **if** flag is True **then**
- 22: **# Reuse Memory**
- 23: Retrieve $\mathcal{C}_{\text{box}} \leftarrow \mathcal{M}[c_t]$.
- 24: **else**
- 25: **# New Constraint**
- 26: $\mathbf{u}_{\text{key}} \leftarrow \mathcal{A}_{\text{vlm}}.\text{Perceive}(s_t)$.
- 27: $\mathcal{C}_{\text{box}} \leftarrow \text{Geometry}(\mathbf{u}_{\text{key}})$.
- 28: Update Memory $\mathcal{M}[c_t] \leftarrow \mathcal{C}_{\text{box}}$.
- 29: **end if**
- 30: Sample $a_t \sim \pi_\theta(\cdot | s_t)$ s.t. $a_t \in \mathcal{C}_{\text{box}}$.
- 31: **else if** μ is **Action Guidance** **then**
- 32: $\mathbf{p}_{\text{way}} \leftarrow \mathcal{A}_{\text{vlm}}.\text{GenWaypoint}(s_t)$.
- 33: Compute a_t derived from \mathbf{p}_{way} .
- 34: **end if**
- 35: **end for**

exploration [44], system automation [2], reward generation [46], unified policies [12], and instruction conditioning [38].

B. Pseudocode of AGPS

In Algorithm 1, we present the detailed pseudocode of Agent-guided Policy Search (AGPS).

C. Task description and training details

In this section, we provide the hardware setup, task descriptions, and specific training parameters for each real-world experiment.

Hardware Setup. We conduct all experiments using a 7-DoF Franka Emika Panda robot arm equipped with a standard parallel-jaw gripper. The perception system consists of two cameras: a wrist-mounted **RealSense D405** for high-precision ego-centric RGB-D observations (resolution 848×480) and a side-mounted **RealSense L515** for global view RGB-D observations (resolution 640×480). The entire training and inference process runs on a workstation equipped with a single NVIDIA RTX 4090 GPU. The control frequency is set to 10Hz.

1) **USB Insertion:** This task involves inserting a USB connector into a USB port, as shown in Figure 7(left). This is a high-precision assembly task that requires sub-millimeter accuracy. The robot must align the connector precisely with the port while handling contact forces. The task is initialized with the gripper holding the USB connector. We employ a random reset mechanism where the initial pose of the end-effector is randomized within a range of $\pm 6\text{cm}$ in the x-y plane, $\pm 5\text{cm}$ in the z-axis, and $\pm 0.06\text{ rad}$ in rotation relative to the target pose. The action space is 6-dimensional (delta position and delta rotation), as the gripper remains closed throughout the task. We utilize an impedance controller with translational stiffness set to 1800 N/m and rotational stiffness set to 150 Nm/rad to allow for compliant insertion. The specific training parameters are detailed in Table I.

TABLE I: Policy training details for the USB Insertion task.

Parameter	Value
Action space	6-dimensional (End-effector delta pose)
Observation space	RGB-D images + Proprioception
Initial offline demonstrations	20
Max episode length	400
Control Frequency	10 Hz
Reset method	Random Reset
Randomization range	$\pm 6\text{cm}$ (XY), $\pm 5\text{cm}$ (Z), $\pm 0.06\text{rad}$ (RZ)
Translational Stiffness	1800 N/m
Rotational Stiffness	150 Nm/rad

2) **Chinese Knot Hanging:** This task involves hanging a soft, deformable Chinese knot onto a hook, as illustrated in Figure 7(right). This task challenges the robot's ability to manipulate deformable objects where the object's state is not fully rigid and can swing or deform during motion. The robot starts holding the knot string. The goal is to navigate the string over the hook successfully. Similar to the USB task, the initial position is randomized to ensure robustness. The action space is 6-dimensional (delta position and delta rotation). Due to the deformable nature of the knot, we adjust the impedance parameters to prevent excessive tension. The detailed parameters are listed in Table II.

D. Query vision language model

To implement the modules of AGPS, we design specific prompt templates that map visual observations directly to structured robotic commands. For the experiments conducted in this work, we use Qwen3-VL-235B-A22B-Instruct [4].

We provide the four core templates used in our experiments:

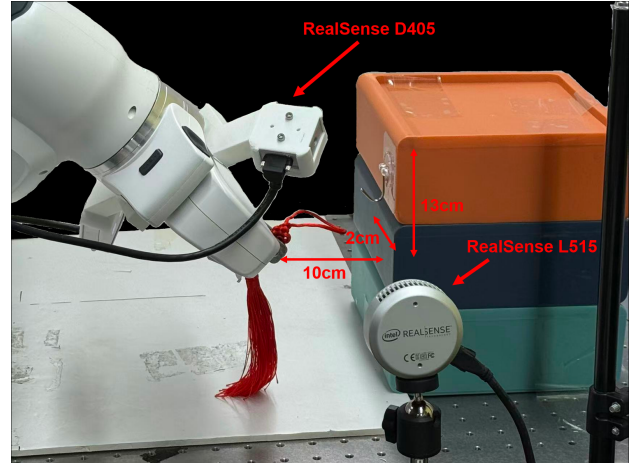
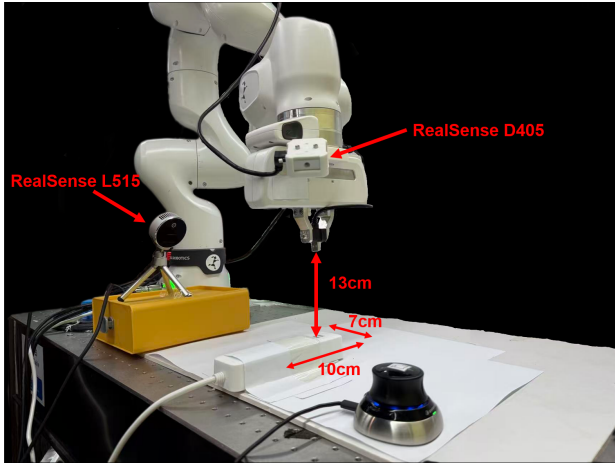


Fig. 7: The workspace of real-world tasks. The Franka gripper is randomly initialized within the areas denoted by the red boundaries and annotations at the beginning of each episode.

TABLE II: Policy training details for the Chinese Knot Hanging task.

Parameter	Value
Action space	6-dimensional (End-effector delta pose)
Observation space	RGB-D images + Proprioception
Initial offline demonstrations	20
Max episode length	200
Control Frequency	10 Hz
Reset method	Random Reset
Randomization range	$\pm 2\text{cm}$ (X), $\pm 2\text{cm}$ (Z)
Translational Stiffness	2000 N/m
Rotational Stiffness	150 Nm/rad

- 1) **Strategy Selection Template:** Corresponds to the DecideMode module. It takes the task description and current image as input to determine whether the agent should perform *Action Guidance* or *Exploration Pruning*.
- 2) **Detect Keypoints Template:** Corresponds to the Perceive module. It identifies task-relevant semantic keypoints (e.g., gripper, target object) in 2D pixel coordinates, which are subsequently projected to 3D space for geometric calculation.
- 3) **Exploration Pruning Template:** Used within the Geometry calculation process. It leverages the VLM's spatial understanding to define a tight, axis-aligned 3D bounding box (C_{box}) based on the detected keypoints, constraining the RL exploration space.
- 4) **Action Guidance Template:** Corresponds to the GenWaypoint module. It generates a sequence of motion primitives (e.g., `move_to`, `lift`) to recover the robot from failure states.

The specific content of these templates is presented below.

Detect keypoints template

You are a precise visual grounding assistant for robotic manipulation tasks.

Task Description:

{task_description}

Your Goal:

Identify the key spatial locations needed to complete this task. For manipulation tasks, this typically includes:

- 1) The robot's end-effector or gripper (the tool that will perform the action)
- 2) The object being manipulated (what the robot is holding or needs to grasp)
- 3) The target location or goal (where the object needs to go)
- 4) Any other critical reference points relevant to task success

Output Format:

Provide keypoints as a JSON array. Use descriptive names that indicate the role of each point in the task.

Coordinate System:

- Use normalized integer coordinates in range [0, 1000]
- Formula:

$$x = \text{round}(\text{pixel}_x / \text{image_width} * 1000),$$

$$y = \text{round}(\text{pixel}_y / \text{image_height} * 1000)$$

Critical Requirements:

- Each keypoint must be located ON a physical object or surface (not floating in space)
- Choose points that are visually distinct and unambiguous

- Include a confidence score (0.0-1.0) based on visual clarity
- Provide a brief description of what the point represents

Output (valid JSON only, no markdown):

```
[
  {
    "name": "descriptive_name",
    "point_2d": [x, y],
    "confidence": 0.95,
    "description":
      "brief description of what
      this point represents"
  },
  ...
]
```

Analyze the image and identify the keypoints needed for this manipulation task.

Strategy selection template

You are a robotic manipulation assistant analyzing the current situation.

TASK: {task_description}

Intervention options:

1) Action guidance:

Directly guide the robot with planned waypoints

- Use when: Large-scale repositioning needed (e.g., moving far from goal, completely wrong region)
- Use when: Coarse motions where precision is NOT critical (e.g., reaching, gross positioning, hanging, placing on large targets)
- Use when: Task involves moving to a clearly visible target with sufficient tolerance (e.g., hanging on hook, placing in large container)
- NOT suitable for: Fine manipulation requiring sub-millimeter precision (insertion into tight holes, threading)
- Effect: Robot executes your planned trajectory step-by-step

2) Exploration pruning

Constrain the exploration region

- Use when: Policy is exploring too widely, wasting time in irrelevant areas
- Use when: Task requires HIGH precision/fine manipulation (tight insertion, alignment with < 5mm tolerance, contact-rich tasks)
- Use when: Robot is near the goal but needs

focused exploration to succeed at a precision task

- Use when: Task involves fitting into tight spaces or requires exact alignment
- Effect: Robot continues learning autonomously, but the workspace is bounded near the goal
- Advantage: Policy learns fine-grained control through trial-and-error in the relevant region

Decision guidelines:

- HIGH precision tasks (USB insertion, threading, tight-fit alignment): Use EXPLORATION_PRUNING
- MODERATE precision tasks (hanging on hook, placing on platform, grasping): Use ACTION_GUIDANCE if repositioning needed
- For coarse repositioning (moving to a different workspace region): Use ACTION_GUIDANCE
- If already near goal AND task needs precision: Use EXPLORATION_PRUNING
- If already near goal AND task is coarse: Use ACTION_GUIDANCE or NO_INTERVENTION

Task precision examples:

- High precision (use exploration_pruning): USB insertion, key insertion, threading needle, screw tightening
- Moderate precision (use action_guidance): hanging on a hook, placing in a bowl, stacking blocks, grasping objects

Instructions:

- 1) Analyze the RGB image showing the current scene
- 2) Identify: Where is the robot? Where is the goal? What precision level is needed?
- 3) Consider: Is this a high-precision task (< 5mm tolerance) or a moderate-precision task (> 1cm tolerance)?
- 4) Decide which intervention strategy is most appropriate

Respond ONLY with a JSON object (no markdown):

```
{
  "strategy": "action_guidance" | "exploration_pruning",
  "reasoning": "Brief explanation (1-2 sentences)"
}
```

Action guidance template

You are a robotics reinforcement learning expert for a Franka arm with a parallel gripper. You are running as a tool-calling agent.

Task: {task_description}

RL goal:

- You are a recovery + curriculum controller for real-world RL.
- Produce a safe primitive sequence to help policy recovery/learning.

You are given:

- 1) One RGB image with labeled keypoints.

Keypoint/target rules:

- A target may be any detected keypoint name or alias (e.g., "ring_kp", "hook").
- Use relative moves carefully and avoid collisions.
- Valid keypoint names for this task:
 - "tcp": current gripper TCP (tool center point)
 - "ring_kp": stable contact point on the held red Chinese-knot loop
 - "hook": contact point near hook tip on the orange box

Available tools/primitives :

- **move_to_pose(target, rpy):** move TCP in a straight line to the target point/pose.
fields:

```
{"name": "move_to_pose",
"target": "<keypoint|above_kp>",
"rpy": [r, p, y] (optional)}
```
- **pre_grasp(target, rpy):** approach/descend near contact.
fields:

```
{"name": "pre_grasp",
"target": "<keypoint|above_kp>",
"rpy": [r, p, y] (optional)}
```
- **move_delta(from, to):** move TCP by delta = to_xyz - from_xyz (base frame).
fields: {"name": "move_delta",
"from": "kp",
"to": "kp"}
Description: move_delta is a straight-line motion in 3D and diagonal moves are allowed. It provides relative displacement primitives to move TCP correctly without specifying TCP as the start or end point.
- **lift(height):** move straight up +z.
fields: {"name": "lift",
"height": 0.05}
- **grasp():** close the franka gripper to close and grasp.

fields: {"name": "grasp"}

- **release():** open the franka gripper to release.

fields: {"name": "release"}

Allowed primitive names: move_delta, lift, move_to_pose, pre_grasp, grasp, release

Agent protocol:

- Output the whole plan in ONE assistant response via tool_calls.
- Use one tool call per primitive step, listed in execution order.
- Do not wait for tool results before producing later steps.
- Avoid manually outputting a primitive JSON list in plain text.
- Put a non-empty analysis string in argument field "analysis" of every tool call.
- You may also include analysis text in assistant content.

Examples:

```
- move_to_pose: {"name": "move_to_pose",
"target": "above_ring_kp"}
- pre_grasp: {"name": "pre_grasp",
"target": "ring_kp"}
- move_delta: {"name": "move_delta",
"from": "ring_kp",
"to": "hook"}
- lift: {"name": "lift",
"height": 0.05}
- grasp: {"name": "grasp"}
- release: {"name": "release"}
```

Notes:

- move_delta moves current TCP by (to_xyz - from_xyz), and diagonal moves are allowed.

Exploration pruning template

You are a precise visual grounding model and a reinforcement learning expert.

Task: {task_description}

Goal:

- **mark the exploration bounding box (explore region) of the franka gripper in the reinforcement learning process, aiming to force the Franka arm to explore the high-value region.**

You are given:

- 1) One RGB image from a fixed camera. This image already has keypoints drawn and labeled. This image has already been annotated with the base world frame coordinates. reference to the image for the base world frame coordinates and

directions.

2) The detected keypoints' 3D coordinates in the robot BASE frame (meters):

```
global_xyz_low: {global_xyz_low}
global_xyz_high: {global_xyz_high}
```

Hard constraints:

- 1) The exploration box should be axis-aligned with the BASE frame axes.
- 2) **The exploration box should be as tight as possible to reduce the exploration space, typically ranging from 0.01-0.02m for the x-axis and y-axis (x and y should not be the same as the goal socket port has different size in the x and y directions).**

Required output format (JSON object):

```
{
  "bbox_3d": [
    x_center, y_center, z_center,
    x_size, y_size, z_size,
    0, 0, 0
  ],
  "debug": {
    "roi_points_used": [
      "tcp", "goal", "..."],
    "margins_m": {
      "x": [neg, pos],
      "y": [neg, pos],
      "z": [neg, pos]
    },
    "clamped_to_global": true/false,
    "reason": "short explanation"
  }
}
```

Now, describe the exploration box suitable for real-world reinforcement learning.